

# Evolution of Low Mass Contact Binaries

K. Stępień<sup>1</sup> and K. Gazeas<sup>2,3</sup>

<sup>1</sup>Warsaw University Observatory, Al. Ujazdowskie 4, 00-478 Warsaw, Poland  
email: kst@astrouw.edu.pl

<sup>2</sup>Department of Astrophysics, Astronomy and Mechanics, University of Athens,  
GR-157 84, Zografos, Athens, Greece

<sup>3</sup>European Space Agency, ESTEC, Mechatronics and Optics Division, Keplerlaan 1,  
2200AG, Noordwijk, The Netherlands  
email: kgaze@physics.auth.gr, kosmas.gazeas@esa.int

## ABSTRACT

We present a study on low-mass contact binaries (LMCB) with orbital periods shorter than 0.3 days and total mass lower than about  $1.4 M_{\odot}$ . We show that such systems have a long pre-contact phase, which lasts for 8–9 Gyrs, while the contact phase takes only about 0.8 Gyr, which is rather a short fraction of the total life. With low mass transfer rate during contact, moderate mass ratios prevail in LMCBs since they do not have enough time to reach extreme mass ratios often observed in higher mass binaries. During the whole evolution both components of LMCBs remain within the MS band.

The evolution of cool contact binaries towards merging is controlled by the interplay between the evolutionary expansion of the less massive component resulting in the mass transfer to the more massive component and the angular momentum loss from the system by the magnetized wind. In LMCB the angular momentum loss prevails. As a result, the orbital period systematically decreases until the binary overflows the outer critical Roche surface and the components merge into a single fast rotating star of a solar type surrounded by a remnant disk carrying excess angular momentum. The disk can be a place of planet formation with the age substantially lower than the age of a host star. The calculated theoretical tracks show good agreement with the physical properties of LMCB from the available observations. Estimates of the frequency of occurrence of LMCB and the merger formation rate indicate that about 40 LMCBs and about 100 low mass merger products is expected to exist within 100 pc from the Sun.

*Planets and satellites: formation – Stars: contact – Stars: eclipsing – Stars: binary – Stars: evolution – Stars: W UMa*

## 1 Introduction – Properties of Contact Binaries

W UMa-type binaries are composed of two cool stars in contact with each other, surrounded by a common convective envelope lying between the inner and outer critical Roche surfaces (Mochnacki 1981). In spite of different component masses they possess almost identical surface brightness. The more massive component of a typical W UMa-type system is a main sequence (MS) star lying not far from the zero age MS (ZAMS) whereas the lower mass component is oversized, sometimes by a factor of several, compared to its expected ZAMS radius (Stępień 2006). They occur in our solar neighborhood with an apparent frequency of one binary among about 500 single stars in the Galactic disk (Rucinski 2006), but their frequency in stellar clusters depends on the cluster age. They have never been observed in open clusters younger than 0.7 Gyr but are ubiquitously found in globular or old open clusters. Their spatial frequency can be as high as 1/45 among blue stragglers in the globular clusters (Rucinski 2000).

W UMa-type systems are considered to be low temperature contact binaries with components of F, G, K spectral type. Hot, massive contact binaries of O and B spectral types are also known but they are surrounded by the common radiative envelope and they seem to have a different origin.

Many thousands of W UMa-type systems are presently known with the majority of them discovered photometrically by the automated sky surveys like OGLE (Szymanski,

Kubiak and Udalski 2001) or ASAS (Pojmanski 2002). However, only about 150 systems have been studied systematically up to date, combining good quality photometric and spectroscopic observations of which a dozen or so has periods shorter than 0.3 d. These data have been published in our older studies. In the current study, they have been updated for a few systems with the new, recently obtained observational data, while a few more systems have been added as a result of the ongoing observational program of W UMa-type stars, in order to increase the sample and cover the entire range of their properties. Following strict selection criteria, only contact binaries with accurate combined solutions based on high quality photometric and radial velocity data for both components have been included in our study. They are listed in Table 1. Solutions based solely on the photometric observations, where the mass ratio is estimated, are not considered to give reliable results. However, we list such binaries in Table 2 as supplementary data. The system GSC 1387:0475 is the only exception in Table 2, as its mass ratio has been determined spectroscopically by Rucinski and Pribulla (2008). They also give the approximate photometric solution stressing, however, that the reliable values of the binary parameters are very difficult to obtain due to a very low orbital inclination of the system. Indeed, the solution given by Yang, Wei and Li (2010) is so much different from the one obtained by Rucinski and Pribulla (2008) that we decided to put the star in Table 2.

Table 1

The list of LMCBs used in the current study, with accurately determined physical parameters (combined photometric and spectroscopic solution)

Name	$P_{\text{orb}}$ [days]	$\log P$	$q_{\text{sp}}$	$M_{\text{pr}}$ [ $M_{\odot}$ ]	$M_{\text{sec}}$ [ $M_{\odot}$ ]	$R_{\text{pr}}$ [ $R_{\odot}$ ]	$R_{\text{sec}}$ [ $R_{\odot}$ ]	$L_{\text{pr}}$ [ $L_{\odot}$ ]	$L_{\text{sec}}$ [ $L_{\odot}$ ]	a [ $R_{\odot}$ ]	$H_{\text{orb}} \cdot 10^{-51}$ [ $\text{g} \cdot \text{cm}^2/\text{s}$ ]	Ref
CC Com	0.2207	-0.6562	0.529	0.720	0.379	0.708	0.522	0.151	0.080	1.585	1.985	1
V523 Cas	0.2337	-0.6313	0.533	0.740	0.381	0.728	0.536	0.139	0.104	1.658	2.096	1
RW Com	0.2373	-0.6247	0.471	0.800	0.380	0.770	0.540	0.260	0.149	1.720	2.202	2
VZ Psc	0.2613	-0.5829	0.800	0.810	0.650	0.780	0.700	0.220	0.124	1.970	3.678	3
44 Boo	0.2678	-0.5722	0.488	0.940	0.470	0.840	0.590	0.573	0.348	2.000	3.123	4
V345 Gem	0.2748	-0.5610	0.142	1.144	0.163	1.103	0.427	1.781	0.313	1.944	1.371	5
BD 07°3142	0.2752	-0.5604	0.662	0.740	0.490	0.810	0.670	0.269	0.229	2.045	2.729	2
BX Peg	0.2804	-0.5522	0.372	1.030	0.383	0.957	0.610	0.639	0.308	2.014	2.853	6
XY Leo	0.2841	-0.5465	0.717	0.813	0.593	0.833	0.714	0.448	0.220	2.036	3.498	1
RW Dor	0.2854	-0.5445	0.703	0.711	0.499	0.832	0.622	0.274	0.181	1.944	2.719	7
BW Dra	0.2922	-0.5343	0.280	0.920	0.260	0.980	0.550	1.085	0.386	1.964	1.853	8
OU Ser	0.2968	-0.5275	0.173	1.109	0.192	1.148	0.507	1.460	0.341	2.041	1.612	9
TZ Boo	0.2972	-0.5270	0.207	0.990	0.210	1.080	0.560	1.240	0.342	1.982	1.593	10

Index ‘pr’ and ‘sec’ stands for the currently observed primary (more massive) and secondary (less massive) component respectively, while the mass ratio is defined as  $q = M_{\text{sec}}/M_{\text{pr}}$ .

1. Zola *et al.* (2010), 2. Djurasevi *et al.* (2011), 3. Hrivnak, Guinan and Lu (1995) 4. Maceroni *et al.* (1981), 5. Gazeas (in preparation), 6. Lee *et al.* (2009), 7. Marino *et al.* (2007), 8. Kaluzny and Rucinski (1986), 9. Zola *et al.* (2005), 10. Christopoulou, Papageorgiou and Chrysopoulos (2011)

All W UMa-type show very similar observational and physical properties. Apparently, they have the same origin and evolution, as shown by Gazeas and Niarchos (2006) and Gazeas and Stępień (2008). According to Bilir *et al.* (2005) the stars have a kinematic age of 5–12 Gyr. This is in agreement with theoretical models, explaining the formation of contact systems by the systematic angular momentum loss (AML) in initially detached binaries with orbital periods of a couple of days, due to the magnetized stellar winds and tidal coupling (Vilhu 1981, 1982, Rahunen 1981, 1982, 1983, Stępień 1995, 2006). Although evolution of binaries towards the contact configuration is quite clear, the evolution during the contact phase and beyond is still controversial, since AML, and mass and energy path exchange between the components lead to differ-

Table 2

The supplemented list of LMCBs used in the current study, for which the mass ratio was determined photometrically

Name	$P_{\text{orb}}$ [days]	$\log P$	$q_{\text{ph}}$	Ref
GSC 1387:0475	0.2178	-0.6619	0.474	1
YZ Phe	0.2347	-0.6295	0.402	2
BI Vul	0.2518	-0.5989	0.692	3
V803 Aql	0.2634	-0.5794	1.000	4
FS CrA	0.2636	-0.5791	0.758	3
BP Vel	0.2650	-0.5768	0.532	5
EK Com	0.2667	-0.5740	0.300	6
V802 Aql	0.2677	-0.5724	0.160	7
IV Dra	0.2680	-0.5719	0.500	8
DD Com	0.2692	-0.5699	0.271	9
FG Sct	0.2706	-0.5677	0.786	10
BM UMa	0.2712	-0.5667	0.540	11
V743 Sgr	0.2766	-0.5581	0.319	12
VW Cep	0.2783	-0.4445	0.400	13,14
V1005 Her	0.2790	-0.5544	0.290	15
AD Cnc	0.2827	-0.5487	0.770	16
V524 Mon	0.2836	-0.5473	0.442	17
ER Cep	0.2857	-0.5441	0.549	18
V700 Cyg	0.2906	-0.5367	0.637	19
V676 Cen	0.2924	-0.5340	0.720	20
V902 Sgr	0.2939	-0.5318	0.120	21
EH Hya	0.2969	-0.5274	0.314	10
ASAS 050837+0512.3	0.2660	-0.5751	0.709	22
ASAS 155906-6317.8	0.2670	-0.5735	0.500	22
ASAS 052452-2809.2	0.2760	-0.5591	0.250	22
ASAS 095048-6723.3	0.2770	-0.5575	0.500	22
ASAS 033959+0314.5	0.2830	-0.5482	0.709	22
ASAS 212915+1604.9	0.2830	-0.5482	0.353	22
ASAS 195350-5003.5	0.2870	-0.5421	0.709	22
ASAS 061531+1935.4	0.2880	-0.5406	0.353	22
ASAS 085710+1856.8	0.2910	-0.5361	0.353	22
ASAS 143751-3850.8	0.2920	-0.5346	0.500	22
ASAS 120036-3915.6	0.2930	-0.5331	0.250	22
ASAS 144243-7418.7	0.2950	-0.5302	0.250	22
ASAS 050852+0249.3	0.2960	-0.5287	0.353	22
ASAS 155227-5500.6	0.2980	-0.5258	0.709	22
ASAS 174655+0249.9	0.3000	-0.5229	0.353	22

1. Rucinski and Pribulla (2008), 2. Samec and Terrell (1995), 3. Bradstreet (1985), 4. Samec, Su and Dewitt (1993), 5. Lapasset, Gomez and Farinas (1996), 6. Samec, Carrigan and Padgen (1995), 7. Samec, Martin and Faulkner (2004), 8. Robb (1992), 9. Zhu *et al.* (2010), 10. Maceroni and van't Veer (1996), 11. Samec, Gray and Garrigan (1995), 12. Samec, Carrigan and Wei Lool (1998), 13. Khajavi, Edalati and Jassur (2002), 14. Binnendijk (1966), 15. Robb, Greimel and Oulette (1997), 16. Qian *et al.* (2007), 17. Samec and Loflin (2004), 18. Maceroni, Milano and Russo (1984), 19. Niarchos, Hoffmann and Duerbeck (1997), 20. Gray, Woissol and Samec (1996), 21. Samec and Corbin (2001), 22. Pilecki and Stepień (2012).

ent evolution than the one we currently know for single stars. The thermal relaxation oscillation (TRO) model, described by Lucy (1976), Flannery (1976) and Webbink (1977), and later developed by a number of authors (Yakut and Eggleton 2005 and references therein), assumes that each component of the binary is out of thermal equilibrium and its size oscillates around the inner Roche lobe. The low mass component is oversized due to the convective energy transfer from the massive component. The binary spends a part of its life in contact and the rest as a semi-detached binary, slowly evolving towards an extreme mass ratio system. An alternative evolutionary model of cool contact binaries has been developed by Stępień (2004, 2006, 2009) and will be presented in more detail in Section 3. Briefly, the model assumes that mass transfer occurs with the mass ratio reversal, similarly as in Algol-type binaries, following the Roche lobe overflow (RLOF) by the massive component. The contact configuration is formed immediately after that or after some additional AML. Each component is in thermal equilibrium and the large size of the currently less massive component results from its advanced evolutionary stage (its core is hydrogen depleted). The energy flows from the presently massive component in a form of the large scale, steady circulation of high entropy matter bound to the equatorial region and encircling the low mass component.

Crucial for the further evolution in contact is the ratio of the AML time scale to the evolutionary time scale of the initially more massive component (Stępień 2011). Its value determines the evolutionary stage of the massive component when it reaches RLOF and transfers rapidly mass to its companion. We consider three different cases: the massive component reaches RLOF when it is still on MS but not yet approaching TAMS, when it is close to, or slightly beyond TAMS, and when it is on the subgiant branch, approaching the red giant branch. Note that no sharp limit occurs between the first and second case, as well as between the second and third case. The transition is continuous so the assignment to the particular case results from the evolutionary behavior following RLOF. In analogy with the terminology introduced by Kippenhahn and Weigert (1967) for the upper MS binaries we will call Case A, AB and B the three above described situations.

Case A rapid mass exchange results in a binary composed of two MS stars with the presently less massive component (donor) being more advanced evolutionary than the accretor. That happens for low mass binaries with short initial periods. After the rapid mass transfer in Case AB the donor is completely, or nearly completely depleted of hydrogen in its center but it has not yet built a significant helium core. It leaves MS and enters the subgiant branch. This is associated with a relatively faster expansion than during the MS phase, which results in a higher mass transfer rate. This prevents the orbit from a rapid shrinking caused by AML and gives the donor enough time to transfer almost all its mass to the accretor. The mass ratio reaches the extreme value leading to the Darwin instability and merging of both components. In Case B RLOF occurs when the star is already approaching the red giant branch and possesses a small helium core of a few tenths of the solar mass. This happens in binaries with long orbital periods. The rapidly expanding star fills its critical Roche lobe when the orbit is still wide and the rapid mass exchange results in formation of an Algol-type binary with the donor being a red giant or subgiant.

In this study we concentrate on contact binaries formed as a result of Case A mass transfer in binaries with the initial period between 1.5 and 2.5 d, (Stępień 2011), and the initial mass of the massive component low enough that its MS life time is longer than the AML time scale. Contact binaries formed following RLOF in Case A will be called low mass contact binaries (LMCB). The slow expansion of the primary results in a moderate mass transfer and thus does not lead to widening of the orbit. In the long run AML prevails, leading to the overflow of the outer critical Roche lobe and the

coalescence of both components when the mass ratio is still moderate.

## 2 The Low Mass Contact Binaries

LMCBs can be distinguished observationally by their very short orbital periods ( $P_{\text{orb}} \leq 0.3$  d), moderate mass ratios ( $0.2 \leq q \leq 0.8$  with a strong concentration around 0.5) low component masses (individually between  $0.2\text{--}1 M_{\odot}$  and totally between  $1.0\text{--}1.4 M_{\odot}$ ) and radii equal to the MS objects. There may be a few exceptions with parameters outside of these limits, nevertheless the great majority of LMCBs have parameters within the above ranges. Their components have late spectral types (G to K) and consequently they show low surface temperatures (4000–5000 K). Such stars are expected to be magnetically very active with cool star spots covering a significant – but strongly variable – fraction of their surface. As a result, their light curves vary on a time scale of years, showing often asymmetry known as O’Connell Effect. In some rare cases their variation is noticed within a few months or even weeks (Gazeas, Niarchos and Gradoula 2006). In almost all LMCBs the massive component shows lower apparent surface brightness than its companion. This is explained by a large coverage of its photosphere with cool, dark spots reducing significantly its apparent luminosity (Eaton, Wu and Rucinski 1980, Stępień 1980, Hendry, Mochnacki and Collier Cameron 1992). Photometrically this effect illustrates the so-called W-phenomenon (Binnendijk 1970) according to which the photometric minimum of light variation occurs when the less massive component is eclipsed, not the more massive one, as normally expected (A-phenomenon). The vast majority of LMCB shows the W-phenomenon, which often confuses the observers on which component is the more massive and which is the less massive one.

The undisturbed photometric temperature of the more massive component is very likely higher than the temperature of the low mass component, as the recent modeling of high quality observations shows (Zola *et al.* 2010). Because the spottiness varies in time, some stars may migrate from W-type to A-type and *vice versa*. Apparently, this migration does not occur among LMCB or occurs only exceptionally.

In agreement with their mass and their late G and K spectral type, LMCB are intrinsically faint. This is the reason why the number of such systems with well determined parameters is very limited. Rucinski (2007) argues, however, that the period distribution of the volume limited sample of W UMa-type systems has a maximum around 0.27 days, *i.e.*, within the range of LMCB. So, in reality, they must be quite numerous in space. Also, according to the results by Bilir *et al.* (2005) they belong to the oldest population of contact binaries, with the kinematic age of 9 Gyr. Recently, Pilecki (2009) obtained photometric solutions for about 2900 eclipsing binaries with good light curves from the sky survey ASAS (Pojmowski 2002). To automate the process, he solved each light curve for several pre-defined values of mass ratio and selected the solution best representing the observed curve. Because of the relatively coarse pre-defined grid, the obtained mass ratios of the analyzed binaries are not distributed continuously but, instead, are grouped at several specified values. In spite of the low accuracy of the mass ratio determinations, his results for contact binaries with periods shorter than 0.3 d show that they all fit well into our criteria for LMCB: their mass ratios lie between 0.25 and 0.8 (see Table 2) and they all show the W-phenomenon.

## 3 Theoretical Background and the New Model

Several theoretical models were proposed to explain the characteristics of contact binaries (CBs), with only a few able to explain the most characteristic observational data.

There are several assumptions in these models, which were made mainly due to the lack of observational evidence or a very limited sample of analyzed CBs. Independent sets of evolutionary models of single stars, produced by many authors, show significant discrepancies, particularly in radius vs. time, time scales to reach a given evolutionary stage *e.g.*, to build a helium core of a given mass etc. Such uncertainties must also exist among programs modeling evolution of close binaries towards the contact phase.

Nevertheless, all models show that both components of a close binary, evolving later into a CB, should lie inside their Roche lobes for some time at early evolutionary phases. When the orbital AM becomes low enough, one or both components will eventually overflow their inner Roche lobes, resulting in a contact configuration with a common envelope around the whole system.

Cool CBs are among the binary systems with the highest level of chromospheric-coronal activity. Therefore, they lose AM and mass by the magnetized wind, just as it is observed in single, highly active stars. In addition, the existing models of CB assume that the low mass component (donor) transfers mass to its companion (accretor) on the evolutionary time scale. The relative rates of all these processes determine the course of binary evolution till merging of both components. In particular, the mass transfer, resulting from the evolutionary expansion of the donor, acts in the direction of the orbit widening. In the absence of AML, the orbital period increases at a rate determined by the condition that the donor overfills its Roche lobe by a narrow margin. The resulting mass transfer rate is rather low, as observed in classical Algols with periods longer than a week, where the AML rate by the magnetized wind is low. However, CBs with periods shorter than 1 day have high AML rates, which changes the situation radically. The AML acts in the direction of shrinking the orbit and both Roche lobes. When the contracting Roche lobe moves deeper beneath the donor surface, the mass transfer rate increases, widening the orbit again. The equilibrium rates of both processes depend on many details of which very important is the evolutionary advancement of the donor. In LMCBs its expansion results from evolution across MS, which is rather slow, hence AML dominates bringing the binary to coalescence before the mass ratio becomes very low. In binaries which are past mass exchange in Case AB or B, donors expand much faster forcing a high mass transfer rate. This prevents the binary from overflowing the outer critical surface in the early phase of the mass transfer process, so the merging of both components will occur only when the extreme mass ratio  $q \leq 0.1$  is reached.

Based on the observational data and the fact that the TRO model encounters several difficulties (Webbink 2003, Stępień 2011, and references therein) a new, alternative model has been suggested by Stępień (2006, 2009; see also Gazeas and Stępień 2008). The main features of this model are:

1. Cool CBs evolve from detached binaries with initial periods close to 2 days.
2. Both components are magnetically active, at the highest, so called saturation, level.
3. Strong magnetized winds blow from both components leading to mass and AM loss. With the full spin-orbit synchronization, the orbital AM is ultimately reduced.
4. Evolutionary expansion of the massive component, together with orbit shrinkage, results in RLOF followed by the rapid mass transfer to the low mass component.
5. The rapid mass exchange proceeds until the mass ratio reversal, similarly as in Algol-type binaries.
6. Depending on the detailed values of the orbital parameters, either a CB emerges directly from the rapid mass exchange phase, or a near-contact binary is formed, which reaches contact after some additional AML.
7. Further evolution of the binary in contact proceeds under the influence of AML and slow mass transfer from the present, evolutionary advanced, low mass com-

ponent (donor) to the present massive component (accretor).

8. At the end, both components merge together forming a single, rapidly rotating star.

Perhaps the most important feature of the present model, differing it from TRO model, is listed under item (5). TRO model assumes that the matter flowing from the more massive, hence hotter, component covers the low mass component completely. The blanket of high entropy gas blocks its core energy flux, which instead of being radiated into space, heats up the convection zone until the specific entropy equals that of the covering matter. The increased entropy makes the convection zone expand until the star fills its Roche lobe. It was shown, however, that the flow of matter from the hotter component is a dynamical process (Tassoul 1992, Stępień 2009). The resulting stream is bound to the equatorial region by the Coriolis force and the low mass component can radiate freely its core energy from the polar regions not covered by the hot matter. Its global parameters, including the radius, change very little, compared to a single star of the same mass. Apart from a temporary loss of thermal equilibrium, the rapid mass transfer following RLOF by the massive component of a close binary will result in a reversal of the mass ratio.

Starting from the initial conditions the following set of equations is solved for each time step

$$\frac{dH_{\text{orb}}}{dt} = -4.9 \times 10^{41} (R_1^2 M_1 + R_2^2 M_2) / P, \quad (1)$$

$$\dot{M}_{1,2} = -10^{-11} R_{1,2}^2, \quad (2)$$

$$P = 0.1159 \cdot a^{3/2} M^{-1/2}, \quad (3)$$

$$H_{\text{orb}} = 1.24 \times 10^{52} M^{5/3} P^{1/3} q (1+q)^{-2}, \quad (4)$$

$$\frac{r_1}{a} = \frac{0.49 \cdot q^{2/3}}{0.6 \cdot q^{2/3} + \ln(1+q^{1/3})}, \quad (5)$$

$$\frac{r_2}{a} = \frac{0.49 \cdot q^{-2/3}}{0.6 \cdot q^{-2/3} + \ln(1+q^{-1/3})}. \quad (6)$$

Here  $t$  is time in years,  $P$ ,  $H_{\text{orb}}$  and  $a$  are the orbital period (in days), orbital AM (in cgs units) and semi-axis (in solar units),  $M_{1,2}$  and  $R_{1,2}$  are masses and radii of both components also in solar units, and  $M = M_1 + M_2$ . Just for reference, the solar spin AM is  $H_{\odot} = 1.63 \times 10^{48}$  in cgs units. From now on, the subscript '1' will denote the initially more massive component and the subscript '2' the initially less massive component so that the initial mass ratio  $q \equiv M_1/M_2 > 1$  but after the rapid mass exchange  $q < 1$ . To allow for the effect of the activity supersaturation  $P \equiv 0.4$  d is adopted in Eq. (1) for periods shorter than 0.4 days. The relations  $R_1(t)$  and  $R_2(t)$ , taken from the evolutionary models of single stars computed by Girardi *et al.* (2000) and Sienkiewicz (see Stępień 2006), supplement the model.

Eqs. (5–6) give approximate sizes of the Roche lobes of both components  $r_1$  and  $r_2$  (Eggleton 1983). For contact configurations these sizes are assumed to be identical with stellar radii.

We assume in the current model that cool CB systems evolve from initially detached configurations with stellar parameters corresponding to ZAMS and orbital periods close to 2 days. Evolution is split in three phases: the detached phase I, until the RLOF by star '1', the rapid mass exchange phase II and the slow mass transfer phase III, which lasts until the presumed merging of the components. To simplify computations, the constant mass transfer rate in phase III is assumed. It is so adjusted that the evolutionary radius of the donor (star '1') is close to the size of its Roche lobe during the whole phase III.

Nothing spectacular happens during phase I – the system simply loses mass and AM *via* the winds while the components slowly expand due to their evolution across the MS. Phase I is described for several binaries in detail by Stępień (2011). Phase II begins when the period is well below 1 day. This phase is very short compared to two other phases. Some mass (and AM) may be lost during it but allowing for them adds two more free parameters to the model, which we want to avoid, so the present calculations are made assuming the conservative mass exchange. Then the system enters phase III when the stars reach contact and evolve as a contact binary.

## 4 The Results of Calculations and Comparison with Observations

The observations put constraints on the initial parameter values of the binaries which evolve later into LMCB. The presently observed total mass range of LMCB restricts the values of the initial total mass to the range  $1.1\text{--}1.6 M_{\odot}$ , because the expected total mass loss due to the winds is around  $0.1\text{--}0.2 M_{\odot}$ . The observed values of the donor radii (star '1') suggest that the stars are close to TAMS and hydrogen in their cores is substantially depleted. This means that they must have been close to TAMS already at RLOF because the following evolutionary phases last much shorter than phase I (see Table 3). This requires that  $M_{1,\text{init}}$  can not be lower than  $0.9 M_{\odot}$  for the metal abundance characteristic of old disk and lower than  $0.8 M_{\odot}$  if the star is metal-poor. Keeping in mind, on the other hand, that the initial total mass should be less than  $1.6 M_{\odot}$  we put a condition  $M_{1,\text{init}} \leq 1.1 M_{\odot}$  to avoid extreme initial mass ratios for which the assumption of the conservative mass transfer in phase II is most likely not fulfilled.

A set of evolutionary models of cool close binaries with different initial conditions was calculated by one of us (Stępień 2011). Time evolution of 27 new models was followed, with initial orbital periods of 1.5, 2.0 and 2.5 days and initial components masses  $1.3+1.1$ ,  $1.3+0.9$ ,  $1.3+0.7$ ,  $1.1+0.9$ ,  $1.1+0.7$ ,  $1.1+0.5$ ,  $0.9+0.7$ ,  $0.9+0.5$  and  $0.9+0.3$  (in solar units). Table 3 gives the details of the models evolving into LMCBs. After the rapid mass exchange (phase II) the constant mass transfer rate was adopted for phase III. Its value was adjusted to keep the radius of the donor within a few percent of the size of its Roche lobe at the beginning and the end of phase III. The donor radius was interpolated using the set of evolutionary models of single stars with different masses. Taking into account the decrease of the donor mass and its evolutionary effects during phase III, the value of the radius at each time step was obtained from the interpolation in time and mass. In most cases the donor radius deviated from the size of its Roche lobe by no more than 10% over the whole phase III. In a few cases, however, keeping a constant mass transfer rate over the whole phase III caused the donor radius to deviate from the size of its Roche lobe by more than 10%. In these cases, phase III was divided into two parts with two different mass transfer rates. End of phase III was signaled by a condition  $q < 0.1$  or when the binary overflowed the outer critical surface.

As it turned out, the most massive binaries with  $P_{\text{init}} = 2.5$  d evolve into short-period Algols with donors possessing a small helium core. This is so because phase I takes more time than the MS life time of  $M_1$  in these binaries (Stępień 2011). RLOF takes place when the donor has already left MS on its way to the red giant branch, which results in a high mass transfer rate. After phase II it continues a fast expansion and AML rate is insufficient to prevent the binary from orbit widening, so it evolves as classical Algols with constantly increasing period. Binaries with  $P_{\text{init}} = 2$  d evolve into CBs with lower mass transfer rates resulting from the fact that their donors have

been just at, or very close to TAMS at RLOF and do not expand so fast as in previous models. Binaries with  $P_{\text{init}} = 1.5$  d reach RLOF when  $M_1$  is still at a distance from TAMS, so after the rapid mass exchange both components reside on MS. Those are the most compact binaries (particularly when both component masses are low) and with a low mass transfer rate in phase III they merge quickly.

We compare a subset of the above described models, fulfilling the condition  $M \leq 1.6 M_{\odot}$ , with the observations of LMCB. Below, we discuss briefly all such models and we show that only some of them satisfactorily reproduce the observations. These models are then discussed in more details. In the following we denote models with  $M_{1,\text{init}} + M_{2,\text{init}}(P_{\text{init}})$ . Apart from the models presented in Stępień (2011) two additional models characteristic of LMCB have been calculated. These are: 0.9+0.4(2.5) and 0.8+0.3(2.5). The latter binary was evolved assuming a decreased metal content  $Z = 0.001$ .

- Model 0.9+0.3(1.5). The model has the lowest initial AM of all considered. Due to a short period, AML rate is relatively high (see Eq. 1). RLOF occurs after 3.8 Gyr when  $P = 0.27$  d and star '1' is hardly evolved from ZAMS. Very soon after the beginning of the rapid mass exchange the binary overflows the outer critical Roche lobe due to the further fast period shortening. A very high mass and AM loss follows, resulting in coalescence of both components. The model never reaches phase III and no stable contact configuration is formed.
- Model 0.9+0.3(2.0). The model has an evolutionary history very similar to the previous one. RLOF occurs after 4.7 Gyr when star '1' has not yet reached 50% of its MS life. Rapid mass transfer tightens the orbit during phase II so much that the binary overflows the outer critical surface. Again, the model never forms a stable contact configuration.
- Model 0.9+0.3(2.5). The model has a significantly higher initial AM than both previous models and, at the same time, lower AML rate. RLOF occurs after 8.6 Gyr when  $P = 0.35$  d and the star '1' reaches about 70% of its MS life (it would be more if its metal content were lower than solar). The thermal equilibrium radii of both components are always smaller than the outer critical surface during phase II so the binary can survive it and enter phase III. Its details are given in Table 3.
- Model 0.9+0.4(2.5). This is the most massive model with the initial period of 2.5 d which evolves into LMCB with properties similar to observed. Listed in Table 3.
- Model 0.9+0.5(1.5). Due to the higher initial AM, compared to the four previous models, it takes 5.5 Gyr until RLOF, in spite of the very short initial period. The period at RLOF is equal to 0.33 d. Both equilibrium radii are comfortably within the outer critical surface during the rapid mass exchange (the minimum period at phase II is equal to 0.25 d). Listed in Table 3.
- Model 0.9+0.5(2.0). RLOF occurs after 9 Gyr when  $P = 0.39$  d and star '1' reaches about 70% of its MS life. The orbit is wide enough during phase II and the binary enters phase III after the rapid mass exchange. Listed in Table 3.
- Model 0.9+0.5(2.5). High initial AM, together with a low AML rate results in a very long phase I. RLOF occurs only after 13 Gyr. This is much longer than the age of the Galactic disk so the model is rejected from the further discussion.
- Model 0.9+0.7(1.5). RLOF occurs after 6 Gyr when  $P = 0.35$  d and star '1' is almost halfway across MS. In binaries with the mass ratio not far from unity, phase II lasts significantly longer than in binaries with other mass ratios as in this

model where it takes 0.35 Gyr, compared to about 0.1 Gyr in other models. At the end of phase II, when the equilibrium configuration of star '1' recedes into its Roche lobe, star '2' lies well inside its Roche lobe, so we obtain a near contact binary of the Algol type. However, AML dominates in phase III and the period decreases fast. Soon a contact configuration is formed which lasts for a short time, ending with the overflow of the outer critical surface. Listed in Table 3.

- Model 0.9+0.7(2.0). RLOF occurs after 10 Gyr when  $P = 0.41$  d and star '1' is close to TAMS. Similarly as in the previous case, star '2' is within its Roche lobe after phase II, so we obtain again a near contact binary of the Algol type. The system evolves into a contact configuration after about 0.5 Gyr. The period shortens until the overflow of the outer critical surface occurs. Listed in Table 3.
- Model 0.9+0.7(2.5). The initial period is too long for RLOF to occur within the age of Universe so the model was not discussed any more.
- Model 1.1+0.5(1.5). RLOF occurs after 3.4 Gyr when  $P = 0.39$  d and star '1' is about halfway across MS. After additional 0.1 Gyr a contact configuration is formed which exists for almost 1 Gyr. Listed in Table 3.
- Model 1.1+0.5(2.0). RLOF occurs after 5.5 Gyr when  $P = 0.45$  d and star '1' approaches TAMS. Contact is established soon afterwards and it lasts for almost 1 Gyr. Listed in Table 3.
- Model 1.1+0.5(2.5). RLOF occurs after 6.8 Gyr when  $P = 0.91$  d and star '1' is already a subgiant with a significant helium core. The binary evolves into Algol with systematically increasing period. The model was excluded from further discussion.
- Model 0.8+0.3(2.5). This is the model with the lowest total mass considered by us. In contrast to the previous models we assumed here the decreased metal content  $Z=0.001$ , so that star '1' evolves faster than the solar composition model of the same mass. RLOF occurs after 11 Gyr when  $P = 0.47$  d and star '1' approaches TAMS. Following the rapid mass transfer a near contact binary is formed, which evolves into a contact configuration after additional 0.7 Gyr. It stays in contact for 0.6 Gyr until coalescence occurs. Listed in Table 3.

The above examples show that LMCBs are formed from binaries with the initial values of parameters lying within quite narrow intervals. Binaries with the low initial total mass – less or equal to  $1.3 M_{\odot}$ , and the initial orbital periods between 1.5 and 2 days do not survive phase II. RLOF occurs when both components are still close to ZAMS so the binary is very compact and the rapid mass exchange results in the immediate merger due to the overflow of the outer critical surface followed by the very fast mass and AM loss from the system. Low initial mass binaries evolve into LMCB only if the initial orbital period is equal to 2.5 days. The binaries with longer periods (of 3 days or more) have so low AML rates in phase I that RLOF occurs after the time longer than the Hubble time. Binaries with high total initial mass of  $1.4$ – $1.6 M_{\odot}$  must have short initial orbital periods of 1.5–2 days for RLOF to occur at the right moment, *i.e.*, when star '1' is close to TAMS. For initial orbital periods equal to 2.5 days or more, and  $M_{1,\text{init}} = 0.9 M_{\odot}$ , the duration of phase I in the high mass binaries is again longer than the Hubble time. If, instead,  $M_{1,\text{init}} = 1.1 M_{\odot}$ , RLOF occurs when  $M_1$  is already on its way to the red giant branch, so the rapid mass exchange results in the formation of an Algol-type binary configuration.

It should be stressed again that the present model of the cool close binary evolution does not contain any free parameters. Relaxing this restriction, *e.g.*, by rejecting the assumption of the conservative rapid mass exchange, would certainly broaden the acceptable range of initial parameters leading to the formation of LMCB.

Table 3  
Results of model calculations

Evolutionary stage	Age [Gyr]	$M_1 + M_2$ [ $M_\odot$ ]	$q$	$P_{\text{orb}}$ [days]	$H_{\text{orb}}$ ( $\times 10^{51}$ )
Initial (ZAMS)	0	0.9+0.3	3.0	2.50	4.275
Start RLOF	8.64	0.835+0.292	2.86	0.350	2.051
Start contact	8.74	0.355+0.772	0.46	0.230	2.001
Coalescence	9.42	0.251+0.867	0.29	0.219	1.571
Initial (ZAMS)	0	0.9+0.4	2.25	2.50	5.550
Start RLOF	11.40	0.816+0.382	2.14	0.426	2.740
Start contact	12.20	0.390+0.797	0.49	0.287	2.401
Coalescence	13.00	0.210+0.961	0.22	0.286	1.562
Initial (ZAMS)	0	0.9+0.5	1.80	1.50	5.709
Start RLOF	5.46	0.858+0.487	1.76	0.327	3.230
Start contact	5.66	0.557+0.786	0.71	0.245	3.077
Coalescence	6.24	0.440+0.895	0.49	0.207	2.623
Initial (ZAMS)	0	0.9+0.5	1.80	2.00	6.284
Start RLOF	8.89	0.832+0.478	1.74	0.385	3.278
Start contact	9.39	0.480+0.823	0.58	0.267	2.888
Coalescence	10.50	0.256+1.032	0.25	0.234	1.858
Initial (ZAMS)	0	0.9+0.7	1.29	1.50	7.645
Start RLOF	5.97	0.854+0.672	1.27	0.345	4.336
Start contact	6.44	0.620+0.899	0.69	0.259	3.832
Coalescence	6.71	0.565+0.950	0.59	0.228	3.540
Initial (ZAMS)	0	0.9+0.7	1.29	2.00	8.414
Start RLOF	10.2	0.825+0.653	1.26	0.408	4.348
Start contact	10.9	0.524+0.942	0.56	0.288	3.558
Coalescence	11.9	0.276+1.177	0.23	0.244	2.221
Initial (ZAMS)	0	1.1+0.5	2.20	1.50	6.674
Start RLOF	3.38	1.066+0.492	2.17	0.386	4.084
Start contact	3.48	0.585+0.971	0.60	0.276	3.957
Coalescence	4.46	0.287+1.255	0.23	0.289	2.559
Initial (ZAMS)	0	1.1+0.5	2.20	2.00	7.346
Start RLOF	5.45	1.045+0.487	2.15	0.452	4.201
Start contact	5.84	0.497+1.029	0.48	0.292	3.651
Coalescence	6.63	0.312+1.203	0.26	0.253	2.560
Initial (ZAMS)	0	0.8+0.3	2.67	2.50	3.912
Start RLOF	11.2	0.734+0.290	2.53	0.473	2.040
Start contact	11.97	0.327+0.683	0.48	0.236	1.707
Coalescence	12.55	0.263+0.735	0.36	0.201	1.407

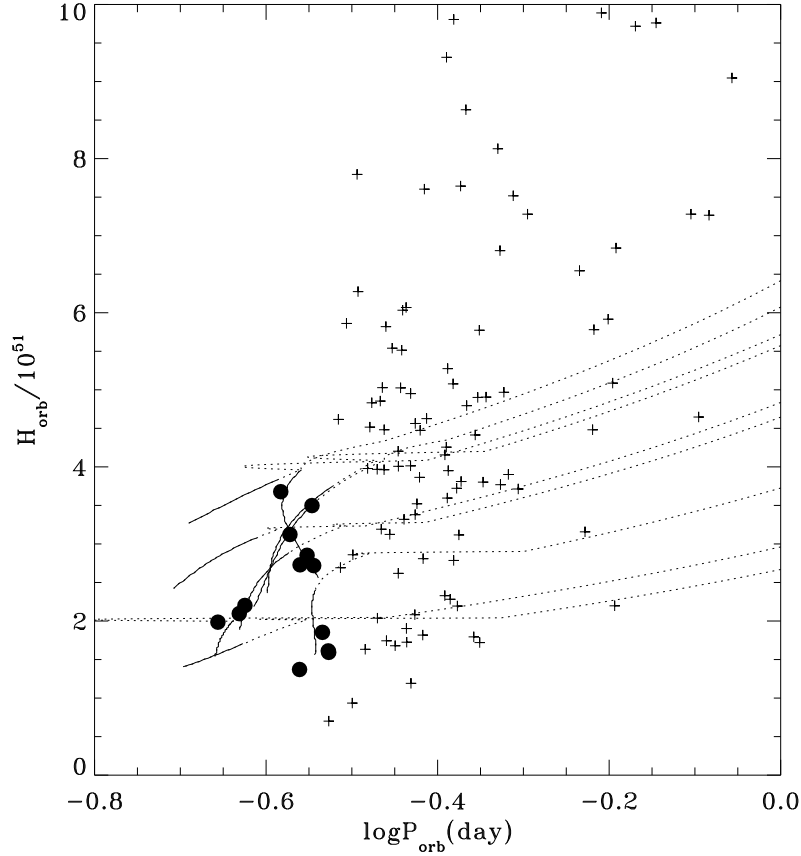


Fig. 1. Comparison of the observed orbital AM of LMCBs from Table 1 – filled circles, and observations of other W UMa-type systems listed in Gazeas and Stępień (2008) – ‘plus’ signs, with the model calculations from Table 3. Solid lines correspond to contact phase and broken lines correspond to earlier phases of the following models (from top to bottom):  $0.9+0.7(1.5)$ ,  $0.9+0.7(2.0)$ ,  $1.1+0.5(1.5)$ ,  $1.1+0.5(2.0)$ ,  $0.9+0.5(1.5)$ ,  $0.9+0.5(2.0)$ ,  $0.9+0.4(2.5)$ ,  $0.9+0.3(2.5)$ ,  $0.8+0.3(2.5)$ .

Figs. 1–4 compare the models with observations. In Fig. 1 the observed period-orbital AM diagram of LMCBs from Table 1 is shown (full circles), together with AM of longer orbital period CBs listed in Gazeas and Stępień (2008) (‘plus’ signs). Overplotted are lines showing the evolution of the orbital AM of the models from Table 3 (dotted lines – phases before contact, solid lines – contact configurations). The orbital period of binaries with high initial (*i.e.*, before the reversal) mass ratios ( $q \approx 2.5-3$ ) goes through the local minimum during phase II. This is shown in Fig. 1 as a loop or hook extending towards short orbital period values. The most prominent one reaches  $\log P = -0.8$  and corresponds to the model  $0.9+0.3(2.5)$ . Its extend suggests that the assumption of the conservative rapid mass transfer may already be violated in this case. As we see, the predicted values of the orbital AM in the contact phase correspond closely to the observed values.

Fig. 2 shows the observed values of the component masses *vs.* orbital period: open and filled circles correspond to more massive and less massive components of LMCBs respectively, while ‘plus’ signs and triangles to the other CBs of our sample. Lines describe the models in the contact phase. Again, as we see, the agreement is excellent.

Fig. 3 gives the observed mass ratio as a function of period. Here, again, the filled circles correspond to LMCBs from Table 1. To strengthen our observation that LMCB avoid extreme mass ratios, we also plotted in Fig. 3 several binaries with periods shorter

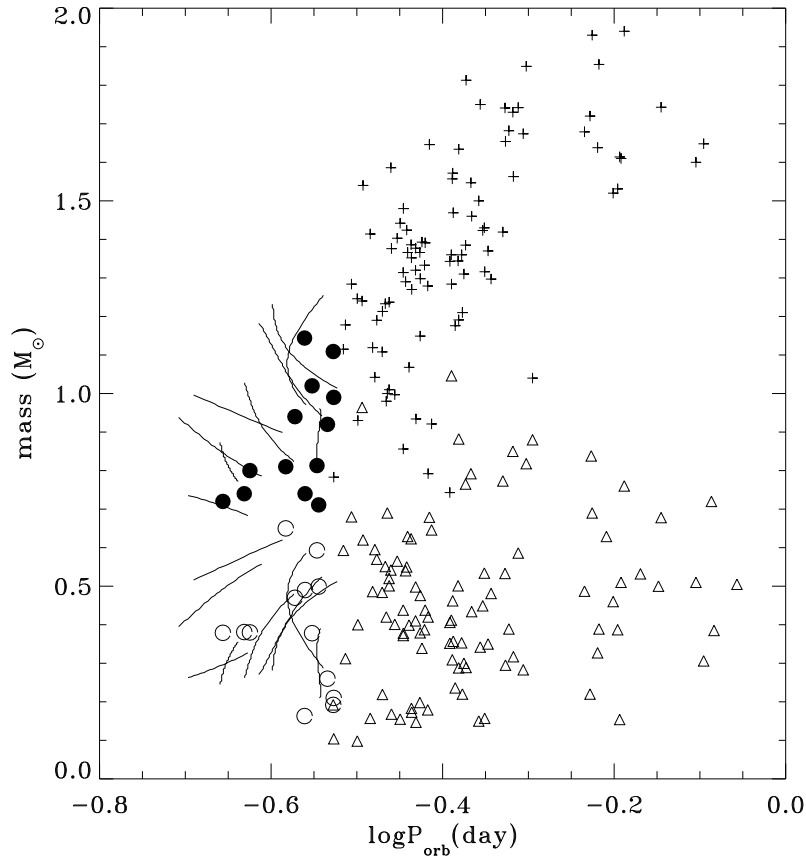


Fig. 2. The observed values of the component masses of LMCBs from Table 1 (open and filled circles) and of other W UMa-type systems listed in Gazeas and Stepień (2008) ('plus' signs and triangles) are compared with the model contact binaries listed in Table 3.

than 0.3 d and mass ratios determined photometrically. These values are considered not to be very reliable, as they lack spectroscopic confirmation or they result from low-quality observational data. These data are given in Table 2 and are plotted as diamonds. The concentration of  $q$  – values around 0.5 for the shortest-period W UMa-type stars has already been noted by Rucinski (2010) in his Fig. 2. Note that none of the computed models extends beyond the orbital period of 0.2 d, because all the considered binaries overflow the outer critical Roche lobe before they reach this value. This prediction agrees very well with the observed short-period limit of W UMa-types stars (Rucinski 2007). As in the previous figures, the observed values are well reproduced by the models, shown here as solid lines.

Fig. 4 shows the mass–radius diagram for the high and low mass components of LMCBs. They are marked with open and filled circles, respectively. Overplotted are evolutionary tracks of models from Table 3. The broken lines denote limits of MS taken from the paper by Girardi *et al.* (2000). Note that the mass of the massive components increases during the evolution in contact whereas the mass of the low mass components decreases. Very good agreement of the observations with the predicted values support the conclusion that LMCB are formed as a result of Case A mass exchange and they finish the evolution in contact when their components are still on MS or, at most, just beyond TAMS.

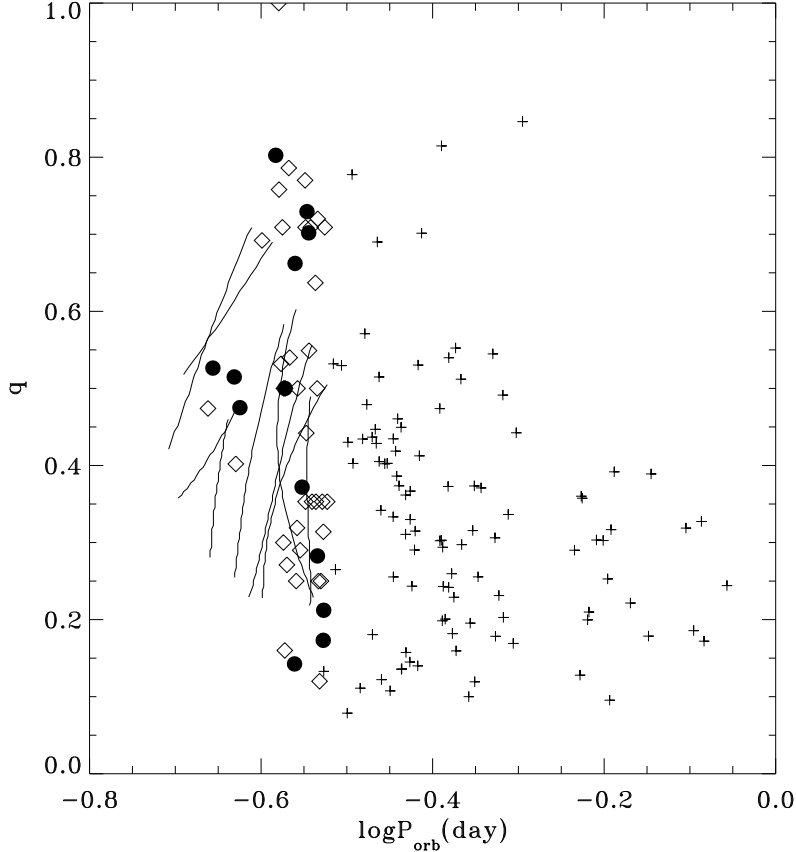


Fig. 3. The observed (spectroscopically determined) values of the mass ratios for the LMCBs listed in Table 1 (filled circles), supplemented by the photometrically determined mass ratios of the LMCBs listed in Table 2 (diamonds) and the other W UMa-type systems listed in Gazeas and Stepień (2008) ('plus' signs) are compared with the evolutionary models (the contact phase) listed in Table 3. Note that some of the diamond signs are grouped at specific values, following the coarse pre-defined search grid (see text).

## 5 Discussion

### 5.1 Total Age and Duration of the Contact Phase

The total age of the models from Table 3 varies from about 4.5 Gyr to 13 Gyr. It depends primarily on the initial mass of star '1'. To produce LMCB, star '1' should be sufficiently advanced evolutionary at RLOF, *i.e.*, its age should reach a considerable fraction of its total MS life time. The latter value is equal to 6.4 Gyr for a  $1.1 M_{\odot}$  star and about 15 Gyr for an  $0.9 M_{\odot}$  star (both for the solar composition). In effect, LMCBs originated from binaries with  $M_{1,\text{init}} = 1.1 M_{\odot}$  cannot be older than about 6 Gyr whereas those originating from binaries with  $M_{1,\text{init}} = 0.9 M_{\odot}$  can be as old as even the Galactic disk. On the other hand, the range of the initial binary parameters leading to LMCB narrows for massive  $M_{1,\text{init}}$  stars. Consequently, only two such models are listed in Table 3. These are:  $1.1+0.5(1.5)$  and  $1.1+0.5(2.0)$ . Binaries with  $M_{1,\text{init}} = 1.1 M_{\odot}$  and  $M_{2,\text{init}} > 0.5 M_{\odot}$ , or with  $M_{2,\text{init}} = 0.5 M_{\odot}$  and original periods longer than 2.0 d do not evolve into LMCB (note that binaries with  $M_{1,\text{init}} = 1.1 M_{\odot}$  and  $M_{2,\text{init}} < 0.5 M_{\odot}$  were not considered here to avoid the non conservative phase II). For  $M_{1,\text{init}} = 0.9 M_{\odot}$  the range of the allowed parameters leading to the formation of LMCBs is broader:  $M_{2,\text{init}}$  can vary between 0.3 and  $0.7 M_{\odot}$ , and the initial period between 1.5 and 2.5 d, except that not all combinations of these parameters are permitted. In particular, to obtain

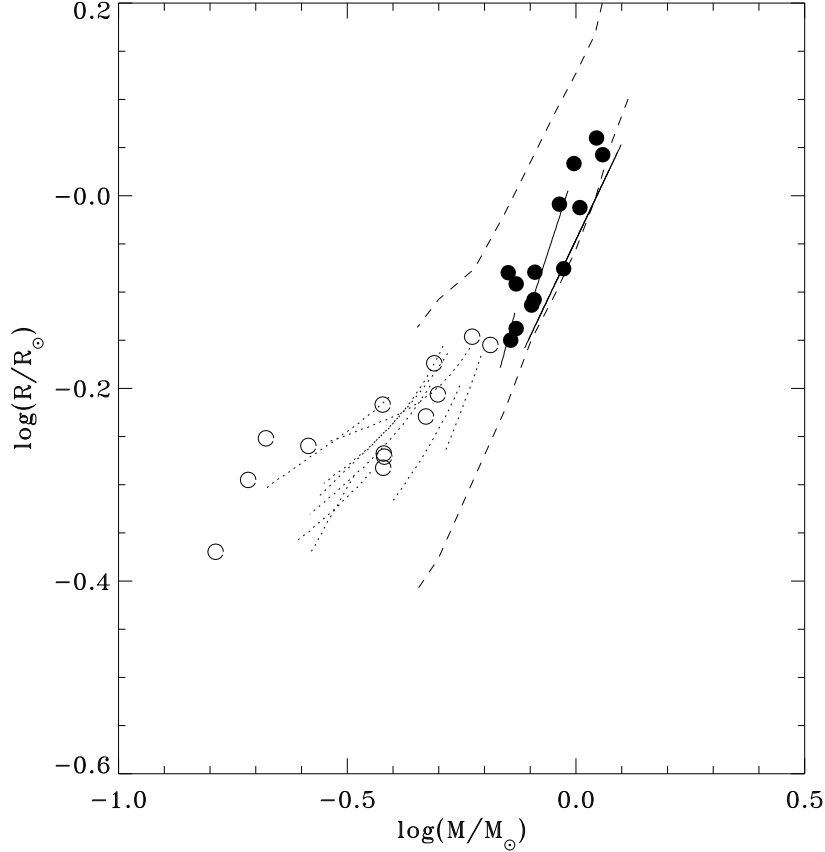


Fig. 4. The mass–radius diagram for the components of the W UMA-type systems from Table 1 (open and filled circles). Evolutionary tracks of the models from Table 3 are overlotted as solid and dotted lines. Note that several solid lines lying along ZAMS overlap with one another. Broken lines show limits of the MS for the solar composition models computed by Girardi *et al.* (2000).

LMCB, the shorter initial period is needed for the more massive  $M_{2,\text{init}}$ . The average age of the models with  $M_{1,\text{init}} = 0.9 M_{\odot}$  is 9.6 Gyr with a dispersion of about 50%. The model  $0.8+0.3(2.5)$  with the decreased metallicity behaves similarly as somewhat more massive models with the solar metallicity.

The duration of the contact phase of the models from Table 3 varies from about 0.3 Gyr to 1.1 Gyr with the average value of 0.6 Gyr. This value depends on the adopted mass transfer rate in phase III. As was mentioned earlier, the mass transfer rate was adjusted so as to make sure that star '1' is close to its Roche lobe at the beginning and the end of phase III, and then its value was kept constant over the whole phase III (with a few exceptions when two different values were used for the initial and final part of phase III). Obviously, the mass transfer rate in real binaries is instantaneously adjusted to keep star '1' slightly exceeding its Roche lobe all the time. The rates used in our model computations can be considered as some sort of means over phase III. They were equal to  $1-3 \times 10^{-10} M_{\odot}/\text{yr}$ , *i.e.*, about 2–3 times less than in other contact binaries (Gazeas and Stępień 2008). The precise duration time of the contact phase is very sensitive to some of the assumptions adopted in the present investigation, as will be discussed in Section 5.2.

The contact phase takes from 4% to 22% of the total age. This percentage is less than 10% for LMCB originating from binaries with  $M_{1,\text{init}} = 0.9 M_{\odot}$  and the highest values are for LMCB originating from binaries with  $M_{1,\text{init}} = 1.1 M_{\odot}$  *i.e.*, those with

a relatively short total age. In some of the considered models the contact phase is preceded by a short semidetached phase when star '1' fills its Roche lobe and transfers mass to star '2' on the evolutionary time scale (past phase II) but star '2' does not yet fill its Roche lobe. An additional AML is needed to form a contact configuration. It is achieved in a fraction of 1 Gyr. This near contact phase can be shortened or completely avoided if a necessary amount of AM is lost during the non conservative phase II. If, however, the rapid mass exchange is conservative, we predict the existence of a population of semidetached binaries with cool components filling their Roche lobe and periods close to but shorter than 0.3 d. Indeed, Pilecki (2009) lists several such binaries detected within the framework of the ASAS program.

Before comparing our final models with observations one should take into account the expected distribution of the initial parameters. Let us assume a flat distribution in  $q$  and  $P_{\text{orb}}$  over the considered interval of the initial parameters, and the Salpeter initial mass function for  $M_{1,\text{init}}$ . A rough estimate of the relative frequency of LMCB originating from binaries with  $M_{1,\text{init}} = 1.1 M_{\odot}$  and from binaries with  $M_{1,\text{init}} = 0.9 M_{\odot}$  or less gives 1/10, *i.e.*, one LMCB out of ten observed should originate from a binary with  $M_{1,\text{init}} = 1.1 M_{\odot}$  and the rest from the binaries with  $M_{1,\text{init}} = 0.9 M_{\odot}$  or slightly less if some of them are metal poor. Correcting the average total age of our models for this factor gives the expected age of about 9 Gyr for the whole population of LMCBs, which is in a very good agreement with the dynamical age of 8.9 Gyr obtained by Bilir *et al.* (2005) for W UMa type binaries with periods 0.2–0.3 days. The weighted mean duration time in contact is 0.8 Gyr.

## 5.2 Space Density of LMCB and the Frequency of Mergers

The observations of LMCBs, together with the present models, make possible an estimate of their space density and the expected rate of merging these binaries into rejuvenated solar type stars (blue stragglers).

Rucinski (2007) analyzed the space distribution of contact binaries with different periods, detected within the ASAS program. He concludes that the density is equal to 14.7 contact binaries with orbital periods between 0.2 and 0.575 days per  $10^6 \text{ pc}^3$ . Of these, 8.2 binaries have periods shorter than 0.3 d, which is about 60% of all W UMa-type stars. This translates into 34 LMCB in the immediate solar neighborhood *i.e.*, in the sphere with the radius of 100 pc. The average life time in contact of LMCB is about 0.8 Gyr (see above). Assuming a stationary situation, 34 LMCB must appear every 0.8 Gyr in this sphere to replace the merging binaries, so the average merging rate is  $34/0.8 \text{ Gyr} \approx 42 \text{ Gyr}^{-1}$ . How many blue stragglers resulting from the coalescence of LMCB is expected in the solar neighborhood? According to our results LMCB are old, with the average age of 9 Gyr, so only few of them were formed earlier than, say 8 Gyr ago. Assuming that the presently estimated rate has existed for the last 2–3 Gyr whereas it was negligible earlier, we come to about 100 solar type mergers lying within 100 pc from the Sun. Mergers resulting from binaries with the extreme initial mass ratio of 3 or more were not included into this order of magnitude estimate but, unless the formation rate of binaries increases rapidly with the increasing mass ratio, including them will not change the result substantially.

Following the coalescence of a binary, an excess AM should be carried away in the form of the excretion disk of which a part will fall again onto the star but the rest may stay as a long living Keplerian disk (Zuckerman *et al.* 2008, Tylenda *et al.* 2011). Such disks can be the place of planet formation (Melis *et al.* 2010, Martin, Spruit and Tata 2011). The planets formed in disks ejected during the coalescence of a contact binary will be much younger than the parent stars (Martin, Spruit and Tata (2011).

### 5.3 Uncertainties

It is known from observations of cool contact binaries that numerous processes and phenomena are present in these systems, which modify their physical parameters and influence their evolution but, so far, are poorly understood and difficult to include into the current models. The light curves of W UMa-type systems show asymmetric maxima (O'Connell effect) interpreted as resulting from dynamical phenomena connected with the mass and energy flow between the components. The shapes of the light curves and the average brightness level vary from one season to another, sometimes with an amplitude comparable to the depth of minima (Rucinski and Paczynski 2002, Gazeas, Niarchos and Gradoula 2006, Pilecki 2009). The apparent surface brightness of the low mass component is higher than that of the massive component in the majority of W UMa-type systems (W-phenomenon), which is contrary to what is expected from simple thermodynamic considerations of the energy transfer between the components. Orbital periods of many (if not all) W UMa-type systems show secular variations. The rates of these variations are statistically distributed symmetrically around zero value and have a distribution well described by a normal curve, indicating their random character (Kubiak, Udalski and Szymanski 2006, Pilecki 2009). Their values are typically very small and are detectable only thanks to their accumulated random-walk deviations. In addition, the majority (if not all) of W UMa-type systems may have companions causing cyclic period variations through the third-body orbital perturbations (Pribulla and Rucinski 2006). It seems that the importance of the period variations for modeling evolution of these stars has often been overstated.

Most of the above mentioned phenomena are closely related to the magnetic activity of the components. This activity does not influence conditions deep in the stellar core, in particular the nuclear energy generation, but it can substantially modify the outer layers and the surface conditions. Suddenly appearing dark spots effectively block a part of the energy flux radiated by a star, which results in an apparent decrease of the stellar brightness and temperature (a disappearance of spots acts in the opposite direction). If spots exist longer than the thermal time scale of the convection zone, the internal structure of this zone is rebuilt. In equilibrium, the whole core energy flux is radiated away but the temperature of the inter-spot photosphere increases as also does the stellar radius (Spruit and Weiss 1986). High level of magnetic activity is the most likely explanation of a systematic difference between the observed and modeled stellar radii of late G, K and M type, rapidly rotating dwarfs. The observed radii show an excess up to 10% compared to models (Torres, Anderson and Giménez 2010). A similar excess is expected in active binaries. None of the existing evolutionary models of cool contact binaries includes this effect properly. It should be stressed here that the rate of evolution in contact depends highly on the accurate values of stellar radii of both components. An ambiguity of several percent can (and probably does) influence the secular mass transfer rate in phase III, hence its duration (see, for example, Eq. (13) in Eggleton and Kiseleva-Eggleton 2002). The basic properties of the presented models and their evolution would not be affected much by ignoring the influence of the magnetic activity, because they result from processes going on deep in the stellar interior. However, surface parameters, like stellar radii, apparent temperatures or the mass transfer rate may depend on the magnetic phenomena. Winds from both components are expected to interact with one another, which can also have an effect on the behavior of a contact binary.

Additional uncertainties are connected with the mass and AM loss model used in this investigation. The uncertainty of the numerical coefficient in the expression for AML rate, given by Eq. (1), is about 30% and that for mass loss rate appearing in Eq. (2) is about a factor of two. The AML rate is saturated in our models for orbital

periods shorter than 0.4 d. This is based on the fact that single stars rotating faster than that show, so called, supersaturation effect, visible in the X-ray flux (Randich *et al.* 1996, Stępień. Schmitt and Voges 2001). Orbital periods of all the contact models discussed in this paper are significantly shorter than 0.4 d. If the higher, unsaturated AML rate applies for these binaries, the duration of phase III could be shorter by a factor of two.

Nonetheless, the basic ingredients of the present model are quite robust because they are based on the well investigated process of stellar evolution and the presence of AML due to magnetized winds. Yet some of the numerical relations and simplified assumptions of our model need to be verified with more accurate data. Till then, the quantitative results of the present paper, in particular the obtained initial parameter range of the progenitors of LMCB and the calculated duration of the contact configuration are susceptible to future refinement.

## 5.4 Conclusions

This work presents the results of modeling the low mass contact binaries (LMCB) and their comparison with observations. It is argued that W UMa-type systems with orbital periods shorter than about 0.3 d have a few common properties which are not shared by their counterparts with longer periods. In particular, they have the total mass lower than  $1.4 M_{\odot}$  and the component masses lower than  $1 M_{\odot}$ , moderate mass ratios clustering around 0.5 with lack of very low values close to, or less than 0.1 and stellar radii placing both components on the MS. They also have low orbital AM – less than  $3 \times 10^{51}$  in cgs units. In addition, a great majority of LMCBs show the W-phenomenon, in contrast to W UMa-type binaries with longer periods where a large fraction of variables show A-phenomenon. LMCBs are intrinsically faint which makes accurate observations difficult. This is why only few have well determined parameters (see Table 1), although they make up majority of all W UMa-type stars in the solar vicinity (Rucinski 2007). If so, they are the main source of mergers producing blue stragglers with properties of MS, solar type stars. After coalescence a circumstellar disk containing the excess AM of the merger is expected to form. It can be the place for planet formation (Melis *et al.* 2010, Martin, Spruit and Tata 2011).

The models of LMCB were obtained from close detached binaries with the total initial masses less than  $1.6 M_{\odot}$  and the initial orbital periods between 1.5 and 2.5 d. Only the proper combination of the initial parameters results in the formation of LMCB. The condition is that the massive component must reach its Roche lobe when it is more than halfway towards TAMS but still some distance to TAMS. If the RLOF occurs when it has not yet evolved from ZAMS significantly, the rapid mass exchange results in an immediate merger of both components with no stable contact phase. If the massive component overflows the Roche lobe when it is close to TAMS, a new born contact binary has a period longer than 0.3 d and it later evolves towards the extreme mass ratio. If RLOF occurs when the massive component has already a small helium core, a short period Algol is formed following the rapid mass exchange. The comparison of model calculations with observations shows a very good agreement between the predicted and observed binary parameters.

The model calculations show that LMCB have the average age of about 9 Gyr although the binary spends most of its life as detached. Duration of the contact phase is rather short – about 0.8 Gyr, *i.e.*, of the order of 10% of the total life. It follows from the observations and our results that about 30–40 LMCBs and about 100 products of the mergers of these stars are expected to exist within 100 pc from the Sun.

Our model describes only the evolution of both components and their orbit. We did not model the energy flow in the contact configuration, so we can not discuss the

component temperatures and, in particular, the W-phenomenon. This problem was discussed at length by Stępień (2009). We only note here that the highest amplitudes of light variations due to the variable spottiness are observed in single stars with masses  $0.7\text{--}0.9 M_{\odot}$ , rotating with periods  $0.2\text{--}0.3$  d (Messina *et al.* 2003). This is just the range where the most of the present primaries of LMCB fit. Very high spottiness of these components may be the reason for the ubiquitous presence of W-phenomenon which is commonly explained as resulting from a heavy coverage of the high mass components by dark spots (Hendry, Mochnacki and Collier Cameron 1992).

The present results are based on a limited number of models with several simplifying assumptions. Many more models with various initial conditions, calculated with the modern evolutionary code of interacting binaries are needed to precisely limit the parameters of the progenitors of LMCB, to reproduce the observed period distribution, to obtain the accurate coalescence rate and to fix the precise mass range of the mergers. Such data have an important significance for the understanding of the planet formation process, particularly the, so called, hot Jupiters.

On the other hand, the good observational data, particularly spectroscopic, are still lacking. The picture is muddled by many biases and selection effects. There are very few systematic surveys, like photometric ASAS or David Dunlap Observatory radial velocity survey carried out by S.M. Rucinski and collaborators. More such data are urgently needed.

**Acknowledgements.** We thank Slavek Rucinski and Wojtek Dziembowski for the very careful reading of the paper, comments and corrections.

## REFERENCES

- Bilir, S., Karataş, Y., Demircan, O., and Eker, Z. 2005, *MNRAS*, **357**, 497.  
 Binnendijk, L. 1966, *Publications of DAO*, **13**, 27.  
 Binnendijk, L. 1970, *Vistas Astron.*, **12**, 217.  
 Bradstreet, D.H. 1985, *Astrophys. J. Suppl. Ser.*, **58**, 413.  
 Christophoulou, P.-E., Papageorgiou, A., and Chrysopoulos, I. 2011, *Astron. J.*, **142**, 99.  
 Djurašević, G., Yilmaz, M., Baştürk, Ö., Kiliçoğlu, T., Latkovi, O., and Çalişkan, Ş. 2011, *Astron. Astrophys.*, **525**, 66.  
 Eaton, J., Wu, C.C., and Rucinski, S.M. 1980, *Astrophys. J.*, **239**, 919.  
 Eggleton, P.P. 1983, *Astrophys. J.*, **268**, 368.  
 Eggleton, P.P., and Kiseleva-Eggleton, L. 2002, *Astrophys. J.*, **575**, 461.  
 Flannery, B.P. 1976, *Astrophys. J.*, **205**, 217.  
 Gazeas, K.D., and Niarchos, P.G. 2006, *MNRAS*, **370**, L29.  
 Gazeas, K.D., Niarchos, P.G., and Gradoula, G.-P. 2006, *Astrophys. and Space Sci.*, **304**, 125.  
 Gazeas, K., and Stępień, K. 2008, *MNRAS*, **390**, 1577.  
 Girardi, L., Bressan, A., Bertelli, G., and Chiosi, C. 2000, *Astron. Astrophys. Suppl. Ser.*, **141**, 371.  
 Gray, J.D., Woissol, S., and Samec, R.G. 1996, *IBVS*, 4359.  
 Hendry, P.D., Mochnacki, S.W., and Collier Cameron, A. 1992, *Astrophys. J.*, **399**, 246.  
 Hrivnák, B.J., Guinan, E.F., and Lu, W. 1995, *Astron. J.*, **455**, 300.  
 Kaluzny, J., and Rucinski, S. 1986, *Astron. J.*, **92**, 666.  
 Khajavi, M., Edalati, M.T., and Jassur, D.M.Z. 2002, *Astrophys. Space Sci.*, **282**, 645.  
 Kippenhahn, R., and Weigert, A. 1967, *Zs. f. Ap.*, **65**, 251.  
 Kubiak, M., Udalski, A., and Szymanski, M. 2006, *Acta Astron.*, **56**, 253.  
 Lapasset, E., Gomez, M., and Farinas, R. 1996, *P.A.S.P.*, **108**, 332.  
 Lee, J.W., Kim, S.-L., Lee, C.-U., and Youn, J.-H. 2009, *P.A.S.P.*, **121**, 1366.  
 Lucy, L.B. 1976, *Astrophys. J.*, **205**, 208.  
 Maceroni, C., Milano, L., Russo, G., and Sollazzo, C. 1981, *Astrophys. Space Sci.*, **45**, 187.  
 Maceroni, C., Milano, L., and Russo, G. 1984, *Astron. Astrophys. Suppl. Ser.*, **58**, 405.  
 Maceroni, C., and van't Veer, F. 1996, *Astron. Astrophys.*, **311**, 523.  
 Marino, B.F., Walker, W.S.G., Bembrick, C., and Budding, E. 2007, *Publ. of the Astron. Soc. of Australia*, **24**, 199.  
 Martin, E.L., Spruit, H.C., and Tata, R. 2011, *Astron. Astrophys.*, **535**, A50.  
 Melis, C., Gielen, C., Chen, C.H., Rhee, J.H., Song, I., and Zuckerman, B. 2010, *Astrophys. J.*, **724**, 470.

- Messina, S., Pizzolato, N., Guinan, E.F., and Rodono, M. 2003, *Astron. Astrophys.*, **410**, 671.
- Mochmacki, S.W. 1981, *Astrophys. J.*, **245**, 650.
- Niarchos, P.G., Hoffmann, M., and Duerbeck, H.W. 1997, *Astron. Astrophys. Suppl. Ser.*, **124**, 291.
- Pilecki, B. 2009, PhD Thesis, Warsaw University.
- Pilecki, B., and Stępień, K. 2012, *IBVS*.6012
- Pojmaski, G. 2002, *Acta Astron.*, **52**, 397.
- Pribulla, T., and Rucinski, S.M. 2006, *Astron. J.*, **131**, 2986.
- Qian, S.-B., Yuan, J.-Z., Soonthornthum, B., Zhu, L.-Y., He, J.-J., and Yang, Y.-G. 2007, *Astron. J.*, **671**, 811.
- Rahunen, T. 1981, *Astron. Astrophys.*, **102**, 81.
- Rahunen, T. 1982, *Astron. Astrophys.*, **109**, 66.
- Rahunen, T. 1983, *Astron. Astrophys.*, **117**, 235.
- Randich, S., Schmitt, J.H.M.M., Prosser, C.F., and Stauffer, J.R. 1996, *Astron. Astrophys.*, **305**, 785.
- Robb, R.M. 1992, *IBVS*.3798
- Robb, R. M., Greimel, R., and Oullette, J. 1997, *IBVS*.4504
- Rucinski, S.M. 2000, *Astron. J.*, **120**, 319.
- Rucinski, S.M. 2006, *MNRAS*, **368**, 1319.
- Rucinski, S.M. 2007, *MNRAS*, **382**, 393.
- Rucinski, S.M. 2010, in "International Conference on Binaries", Eds. V. Kalogera and M. van der Sluys, *AIP Conf. Proc.*, **1314**, p. 29.
- Rucinski, S.M., and Paczynski, B. 2002, *IBVS*.5321
- Rucinski, S.M., and Pribulla T. 2008, *MNRAS*, **388**, 1831.
- Samec, R.G., Su, W., and Dewitt, J.R. 1993, *P.A.S.P.*, **105**, 1441.
- Samec, R.G., Carrigan, B., and Padgen, E.E. 1995, *IBVS*.4167
- Samec, R.G., and Terrell, D. 1995, *P.A.S.P.*, **107**, 427.
- Samec, R.G., Gray, J.D., and Carrigan, B.J. 1995, *P.A.S.P.*, **107**, 136.
- Samec, R.G., Carrigan, B. J., and Wei Looi, M. 1998, *Astron. J.*, **115**, 1160.
- Samec, R.G., and Corbin, S.F. 2001, *IBVS*.5145
- Samec, R., and Loflin, T. 2004, *Observatory*, **124**, 284.
- Samec, R.G., Martin, M., and Faulkner, D.R. 2004, 5527.
- Spruit, H.C., and Weiss, A. 1986, *Astron. Astrophys.*, **166**, 167.
- Stępień, K. 1980, *Acta Astron.*, **30**, 315.
- Stępień, K. 1995, *MNRAS*, **274**, 1019.
- Stępień, K. 2004, in "Stars as Suns: Activity, Evolution and Planets", *IAU Symp.*, **219**, Eds. A.K. Dupree and A.O. Benz, *Astr. Soc. of Pacific*, p. 967.
- Stępień, K. 2006, *Acta Astron.*, **56**, 199.
- Stępień, K. 2009, *MNRAS*, **397**, 857.
- Stępień, K. 2011, *Acta Astron.*, **61**, 139.
- Stępień, K., Schmitt, J.H.M.M., and Voges, W. 2001, *Astron. Astrophys.*, **370**, 157.
- Szymaski, M., Kubiak, M., and Udalski, A. 2001, *Acta Astron.*, **51**, 259.
- Tassoul, J.-L. 1992, *Astrophys. J.*, **389**, 375.
- Torres, G., Andersen, J., and Giménez, A. 2010, *Astron. Astrophys.Rev.*, **18**, 67.
- Tylenda, R., Hajduk, M., Kamiski, T., Udalski, A., Soszynski I., Szymaski, M.K., Kubiak, M., Pietrzyski, G., Poleski, R., Wyrzykowski, ., and Ulaczyk, K. 2011, *Astron. Astrophys.*, **528**, 114.
- Vilhu, O. 1981, *Astrophys. Space Sci.*, **78**, 401.
- Vilhu, O. 1982, *Astron. Astrophys.*, **109**, 17.
- Webbink, R.F. 1977, *Astrophys. J.*, **211**, 881.
- Webbink, R.F. 2003, in "Stellar Evolution", Eds. S. Turcotte *et al. ASP Conf. Ser.*, **293**, p. 76.
- Yakut, K., and Eggleton, P.P. 2005, *Astrophys. J.*, **629**, 1055.
- Yang, Y.-G., Wei, J.-Y. and Li, H.-L. 2010, *New Astronomy*, **15**, 155.
- Zhu, L., Qian, S.-B., Mikulášek, Z., Zejda, M., Zvěřina, and Diethelm, R. 2010, *Astron. J.*, **140**, 215.
- Zola, S., Kreiner, J. M., Zakrzewski, B., Kjurkchieva, D.P., Marchev, D.V., Baran, A., Rucinski, S.M., Ogloza, W. Siwak, M., Koziel, D., Drozd, M., and Pokrzywka, B. 2005, *Acta Astron.*, **55**, 389.
- Zola, S., Gazeas, K., Kreiner, J.M., Ogloza, W., Siwak, M., Koziel-Wierzbowska, D., and Winiarski, M. 2010, *MNRAS*, **408**, 464.
- Zuckerman, B., *et al.* 2008, *Astrophys. J.*, **683**, 1085.